C-Arm CT Measurement of Cerebral Blood Volume and Cerebral Blood Flow Using a Novel High-Speed Acquisition and a Single Intravenous Contrast Injection

K. Royalty, M. Manhart, K. Pulfer, Y. Deuerling-Zheng, C. Strother, A. Fieselmann, and D. Consigny

ABSTRACT

BACKGROUND AND PURPOSE: Assessment of perfusion parameters is important in the selection of patients who are most likely to benefit from revascularization after an acute ischemic stroke. The aim of this study was to evaluate the feasibility of measuring cerebral perfusion parameters with the use of a novel high-speed C-arm CT acquisition in conjunction with a single intravenous injection of contrast.

MATERIALS AND METHODS: Seven canines had experimentally induced focal ischemic regions confirmed by CT perfusion imaging. Four hours after ischemic injury creation, each subject underwent cerebral perfusion measurements with the use of standard perfusion CT, immediately followed by the use of C-arm CT. Cerebral blood flow and cerebral blood volume maps measured by C-arm CT were quantitatively and qualitatively compared with those measured by perfusion CT for 6 of the 7 canine subjects.

RESULTS: Results from independent observer evaluations of perfusion CT and C-arm perfusion maps show strong agreement between observers for identification of ischemic lesion location. Significant percentage agreement between observers for lesion detection and identification of perfusion mismatch between CBV and CBF maps indicate that the maps for both perfusion CT and C-arm are easy to interpret. Quantitative region of interest–based evaluation showed a strong correlation between the perfusion CT and C-arm CBV and CBF maps (R^2 = 0.68 and 0.85). C-arm measurements for both CBV and CBF were consistently overestimated when compared with perfusion CT.

CONCLUSIONS: Qualitative and quantitative measurements of CBF and CBV with the use of a C-arm CT acquisition and a single intravenous injection of contrast agent are feasible. Future improvements in flat detector technology and software algorithms probably will enable more accurate quantitative perfusion measurements with the use of C-arm CT.

ABBREVIATIONS: AIF = arterial input functions; PCT = perfusion CT; TAC = time-attenuation curves

Assessment of the impact of an ischemic insult on brain viability is best performed with the use of physiologic rather than morphologic criteria. This is especially so during the acute phase of an ischemic stroke, when anatomic changes are minimal and the options for revascularization are greater and most effective.[1] Because of limitations in the temporal resolution of angiographic C-arm rotational acquisitions, measurement of cerebral perfusion parameters has required either CT or MR imaging. Recent studies, however, have now demonstrated the feasibility of measuring CBV (in animals and humans) and CBF (in animals) with the use of flat detector C-arm angiographic systems.[2-6]

"Time is brain," but time is not an optimal indicator for selecting patients who are most likely to benefit from revascularization. There is also wide variation in the size and rate of infarct development, depending on many variables, for example, collateral supply, thrombus location and type, and age. In our opinion, these factors combined with the ability to distinguish infarcted brain from ischemic but still viable tissue provide strong motivation to identify techniques that will provide physicians with not only anatomic information but also the physiologic information that is necessary for optimization of patient selection for revascularization within a timeframe in which treatment may be most effective. The angiographic suite provides unparalleled anatomic information; in addition, the ability to obtain measurements of

Received October 18, 2012; accepted after revision January 9, 2013.

From the Department of Biomedical Engineering (K.R.), and School of Medicine and Public Health (K.P., C.S., D.C.), University of Wisconsin, Madison, Wisconsin; Siemens Medical Solutions USA (K.R.), Hoffman Estates, Illinois; Pattern Recognition Lab (M.M.), Friedrich-Alexander University, Erlangen, Germany; and Siemens AG, Healthcare Sector (Y.D.-Z., A.F.), Forchheim, Germany.

Please address correspondence to Kevin L. Royalty, MS, MBA, University of Wisconsin, Department of Biomedical Engineering, 1550 Engineering Dr, Madison, WI 53706; e-mail: kevin.royalty@siemens.com

Indicates open access to non-subscribers at www.ajnr.org

http://dx.doi.org/10.3174/ajnr.A3536

perfusion parameters would seem to create an ideal venue for the diagnosis and treatment of patients with an acute ischemic stroke.

To date, dynamic perfusion imaging with the C-arm angiographic systems has been limited by the slow gantry rotation times, typically on the order of 5–20 seconds. Previous work in both CT perfusion imaging and C-arm CT perfusion imaging demonstrates that temporal resolution in this range is not sufficient to yield accurate results for the measurement of dynamic cerebral perfusion measurements.[7,8] Previous work has demonstrated qualitative and quantitative accuracy of CBV measurements made with the use of C-arm CT in conjunction with a contrast injection protocol aimed at delivering a steady-state of contrast in the parenchyma.[2-5,9-11] Although this method provides information that is helpful in better understanding the viability of ischemic tissue (ie, identifying tissue when autoregulation appears to be intact), it does not provide the ability to distinguish ischemic core from penumbra. Ganguly et al[8] and others[12,13] have recently demonstrated, in a swine model, the feasibility of the use of C-arm CT for dynamic perfusion measurement. Our aim was to further evaluate, in a canine stroke model, the feasibility of performing dynamic cerebral perfusion measurements with the use of a novel high-speed C-arm CT data acquisition in conjunction with a single intravenous (IV) injection of contrast medium.

MATERIALS AND METHODS

Creation of Canine Ischemia and Core Lesion

Under an institutionally approved Animal Care and Use Committee protocol, 7 canines were studied. General anesthesia was introduced with propofol 10 mL/kg IV injection and maintained with the use of 1–5% isoflurane and 100% oxygen. Heart rate, respiration rate, blood oxygen saturation level, end-tidal CO_2 level, and body temperature were monitored and recorded for each subject throughout the duration of the procedure. Initial 2D angiography was performed to verify that cerebral vessels were patent and exhibited normal flow. An ischemic injury was successfully induced in 1 of the cerebral hemispheres in all subjects. Ischemia was created by the use of a 4F catheter (Tempo 4; Cordis, Miami Lakes, Florida) that was placed into either the common carotid artery or the vertebral artery. A microcatheter (FasTracker 18; Target Therapeutics, Fremont, California) was then advanced to the origin of the middle cerebral artery or the internal carotid artery, and embolic material mixed with contrast medium (Avitene; Bio-Medicine, Houston, Texas) was then slowly injected until there was angiographic evidence of stasis of contrast in the arteries of the ipsilateral middle cerebral artery distribution. The Avitene mixture was concentrated to provide a proximal occlusion to avoid only being distributed to the small distal branches of the middle cerebral artery territory.

CT Perfusion Acquisition

Perfusion CT (PCT) imaging was performed 3.5 hours after induction of ischemia by means of a 64-section volume scanner (Discovery CT750 HD; GE Health Care, Waukesha, Wisconsin). An IV injection of iopamidol, 370 mgI/mL (Isovue 370; Bracco, Princeton, New Jersey) was performed with the use of a dual-syringe power injector (Mark V ProVis; Medrad, Indianola, Pennsylvania) with a monophasic injection of 16 mL of contrast at a rate of 2.0 mL/s immediately followed with a 10-mL saline chase with a rate of 2 mL/s. After the injection and after a 5-second prep delay, continuous scanning was initiated with the use of the following parameters: 80 kVp, 200 mA, 1 second per rotation for 50 seconds.

C-Arm CT Perfusion Acquisition

Immediately after the PCT examination, the canine was brought to the angiography suite (Artis Zeego; Siemens, Erlangen, Germany) for C-arm CT perfusion imaging. Identical contrast medium was used for the C-arm CT as was used for the PCT scan. Contrast was injected directly into a peripheral vein with the use of a dual-syringe angiographic power injector (Medtron, Saarbrücken, Germany) at a rate of 3.5 mL/s, with a total volume of 28 mL, immediately followed by a saline chase at a rate of 3.5 mL/s, with a total volume of 10 mL. Before the start of the injection, a series of 2 bi-direction high-speed baseline scans were performed to obtain a baseline set of nonenhanced (mask) images. For the first animal subject, 8 seconds after the start of the peripheral contrast injection, a bi-directional series of 7 sequential high-speed C-arm CT rotational acquisitions was initiated. Data from these rotations were then used to calculate time-attenuation curves (TAC). On review of the results from the initial animal subject, it was determined that the 8-second x-ray delay was too long because there was already significant enhancement of the basilar artery at the time of the initial acquisition. An x-ray delay of 5 seconds was used for the remaining 6 studies. Physiologic parameters monitored during the study did not significantly change between the CT perfusion and C-arm perfusion acquisitions. Canine subjects were euthanized immediately after the C-arm CT acquisitions according to the approved protocol.

The mechanical properties of the robotic C-arm system allow for the design of custom high-speed rotations for CT imaging. For this experiment, a custom high-speed bi-directional acquisition protocol was developed as follows: seven 200° rotations over 2.8 seconds with a 1.5-second pause between rotations (4 forward rotations and 3 reverse rotations). During each rotation, the C-arm system acquires 133 projections at approximately 60 projections per second. Each projection was acquired at 70 kVp and 1.2 μGy/frame dose level, with the automatic exposure control enabled for the duration of the acquisition with a bit-depth of 14 bits. This acquisition protocol resulted in a sampling rate of approximately 4.3 seconds, with a total acquisition duration of 28.6 seconds (excluding the initial 5-second delay).

C-Arm CT Reconstruction of Temporal 3D Datasets

The basic reconstruction process follows a modified version of the algorithm reported by Ganguly et al[8] and Fieselmann et al.[12] Each C-arm CT rotation is first individually reconstructed (by use of a standard filtered back-projection algorithm) resulting in 2 baseline (nonenhanced) volumes and 7 contrast-enhanced volumes, each of which individually represents a composite of the contrast dynamics occurring within each of the seven 2.8 second rotations. An in-plane gaussian kernel (SD = 1 mm) and an axial moving average filter (5 mm) were used to improve the signal-to-noise ratio of the parenchyma. To correct for motion, each recon-

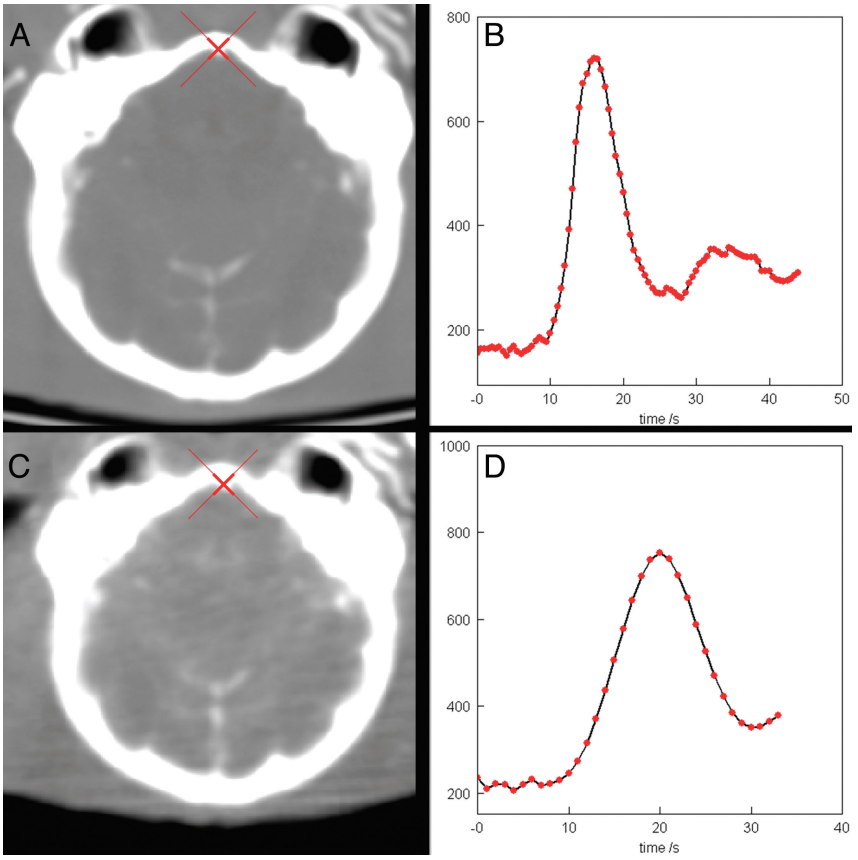

FIG 1. The canine basilar artery was selected as the arterial input function (AIF) reference for all subjects and modalities. *A*, CT section and location of AIF; *B*, TAC for CT AIF location; *C*, C-arm CT section and location of AIF; and *D*, TAC for C-arm CT AIF location.

structed volume was registered with the appropriate baseline volume, that is, forward or reverse. After the motion correction, each voxel was then interpolated to a temporal resolution of 1 volume per second by use of a cubic spline interpolation method and then archived in a standard DICOM CT perfusion format.

Perfusion Data Processing

In an effort to minimize the effect on the measurements as a result of processing the data by use of perfusion software algorithms from 2 vendors,[14] prototype perfusion software (Siemens) was used to calculate the perfusion parameters for both the PCT and C-arm CT datasets. The prototype software consisted of a modified version of the software used by Ganguly et al[8] and Fieselmann et al,[12] which uses a widely accepted deconvolution approach to calculate the dynamic perfusion parameters. To optimize comparison of perfusion maps done on the 2 modalities, C-arm CT and PCT datasets were co-registered.

After co-registration, arterial input functions (AIF) were manually selected in the canine basilar artery (Fig 1). It was chosen as the site of the AIF for 3 reasons. First, the inability to acquire acquisitions with the C-arm in >29 seconds dictated that we use an intracranial vessel rather than an early-filling extracranial vessel to maximize the temporal coverage of the canine's brain enhancement (particularly in the ischemic territory). Second, the multi-section CT orientation made it difficult to obtain section orientations for other intracranial vessels (such as the anterior communicating or middle cerebral arteries) that were not orthogonal to the vessel orientation.[15] Third, the basilar artery has been shown to provide a significant amount of blood flow to the canine cerebral parenchyma.[16] The basilar artery for the canine is approximately 1 mm or less in diameter, which makes it difficult to define the region of interest for the input function in such a way where there is no partial volume effect. To keep the partial volume effects similar between C-arm CT and PCT, the spatial resolution of the reconstructions was kept as similar as possible between the 2 modalities (0.5 mm and 0.6 mm for C-arm and PCT, respectively). A section thickness of 5 mm was used for both modalities.

Qualitative Reader Evaluation

For qualitative analysis of the perfusion maps, 3 experts (2 neuroradiologists and 1 endovascularly trained neurosurgeon with more than 10 years of experience treating cerebrovascular disease) were asked to evaluate 2 series of perfusion maps. The first series of maps was intended to evaluate the independent observer agreement for the identification of an ischemic lesion location within a given perfusion map. The series of maps consisted of both CBV and CBF maps from each of the modalities selected at 2 different nonadjacent section levels (chosen from PCT sections) for each subject (n = 48 total maps from both modalities). For each map, the observers were asked to provide a score of "N" for no lesion, "L" for left hemisphere lesion, "R" for right hemisphere lesion, or "B" for bilateral hemisphere lesion.

The second series of perfusion maps were intended to evaluate the ability for the observers to detect a perfusion mismatch. The observers were presented with a random pair of CBV and CBF maps. Each pair of CBV and CBF maps was from the same technique, the same canine subject, and matched at the same section level. For each pair of maps, the observers were asked to decide if a lesion was present on one or both maps and if there was a mismatch in the size of the lesion, that is, a perfusion mismatch. A mismatch was defined as a difference in the size (area) of the ischemic lesion between the presented CBV and CBF maps. Twenty-four pairs of maps (combined PCT and C-arm CT) were presented to each observer.

The results were then evaluated for interobserver agreement by use of the κ coefficient statistical method.[17]

Quantitative Evaluation

For each technique, CBV and CBF maps (Fig 2) were generated by the prototype and exported in standard DICOM format. Region-of-interest evaluation was performed on a standard syngo X Workplace (Siemens). For each perfusion map, a 0.6-

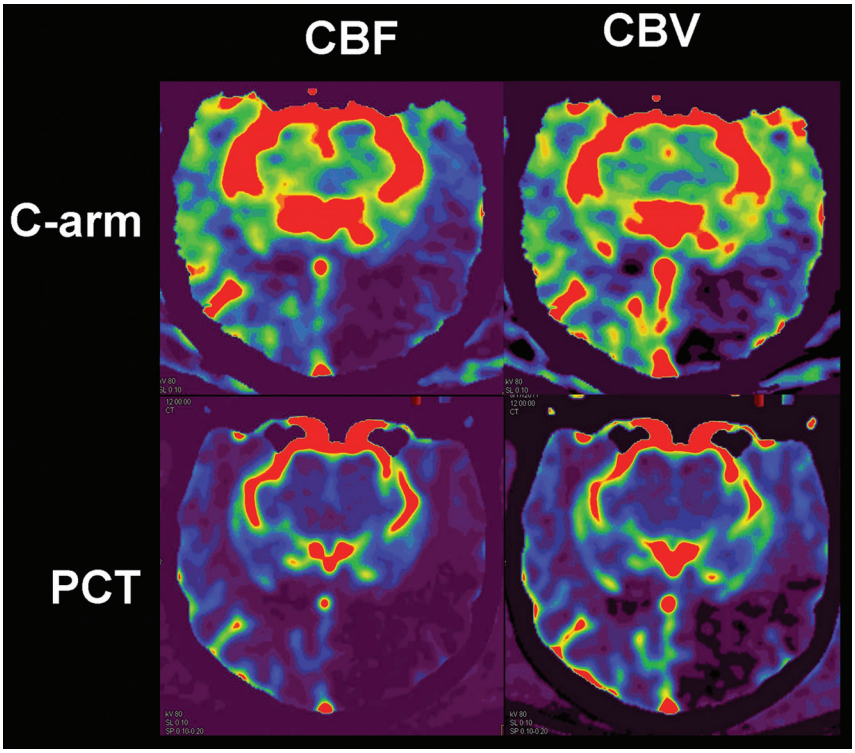

FIG 2. Example of CBV and CBF maps from each technique as presented to the observers. A commercial color map (Syngo PBV Neuro IR; Siemens) was used. All CBF maps used a range of 0–100 mL/100 g/s. All CBV maps used a range of 0–10 mL/100 g.

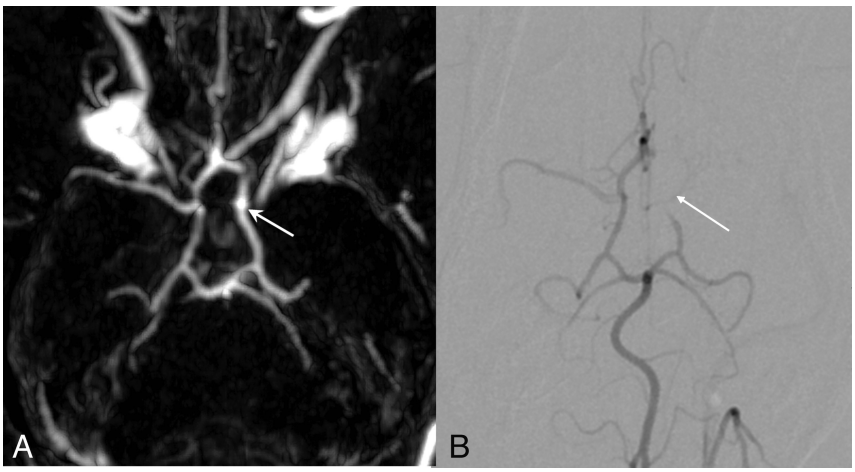

FIG 3. *A,* C-arm CT arterial phase 3D reconstruction show a proximal middle cerebral artery occlusion *(white arrow). B,* Comparison with 2D DSA selective angiogram performed 4 hours earlier also shows a proximal MCA occlusion.

cm^2 region of interest was placed in the center of the ischemic lesion, and a second region of interest was then placed in a symmetric point in the contralateral hemisphere. Care was taken not to include any significant blood vessels within the region circumscribed by the region of interest. This process was performed at 2 different section levels for each subject and for each technique. These perfusion maps were then presented to readers for interpretation and analysis. In addition to the perfusion maps, CTA-like reconstructions were performed with the use of the same datasets (Fig 3).

RESULTS

After review of the results from the first canine, it was determined that an x-ray delay of 8 seconds was too long to capture the rise in arterial enhancement in the basilar artery and thus resulted in a TAC that did not accurately represent the contrast bolus. This resulted in data that were not representative of the other 6 subjects, and, for the purposes of statistical and qualitative analysis, this subject was excluded.

Qualitative Evaluation Results

The combined results of all observers for the lesion detection study are presented in Table 1. Each observer scored a total of 24 randomly presented perfusion maps for each technique. Table 2 presents the statistical results of the κ interobserver agreement evaluation for the lesion detection study.

Table 3 presents the combined observer results from the mismatch detection study. Each observer scored a total of 12 randomly presented section-matched pairs (CBV and CBF) of maps for each technique. Table 4 presents the statistical results of the κ interobserver agreement evaluation for the mismatch detection study.

Quantitative Evaluation Results

For each subject, a region of interest was placed, as closely as possible, in the center of the ischemic lesion; a second region of interest was then placed in a symmetric location in the contralateral hemisphere. This process was performed at 2 different nonadjacent section levels for each subject. Table 5 summarizes the mean values and standard deviations for CBF measurements for each technique. A similar comparison of CBV results is shown in Table 6.

A regression analysis of the C-arm and PCT CBF and CBV region-of-interest measurements indicates an R^2 value of 0.85 for CBF measurements and 0.68 for CBV, indicating a relatively strong correlation for both values. Concordance correlation coefficients were also calculated as 0.56 and 0.39, respectively, for CBF and CBV measurements.

A Bland-Altman analysis was also performed for both the CBV and CBF measurements between the 2 modalities. The results in Fig 4 show that there is a systematic overestimation of both CBF and CBV for the C-arm CT measurements relative to the PCT measurements. The degree of overestimation by C-arm CT is shown to in-

Table 1: Combined observer results for lesion identification and location by modality

	Left	Right	Bilateral	None
C-arm ($n = 72$)	60	12	0	0
PCT ($n = 72$)	49	16	3	4

Note:—n = total number of CBV and CBF perfusion maps presented to all observers per modality.

Table 2: Kappa statistical evaluation for interobserver performance of ischemic lesion detection for 3 independent observers

	κ Coefficient	Percentage Agreement	Statistical Significance
C-arm ($n = 24$)	1.00	100.0%	$P < .01$
PCT ($n = 24$)	0.74	87.5%	$P < .01$

Note:—n = total number of perfusion maps presented to a single observer.

Table 3: Combined observer results for mismatch identification by modality

	CBV/CBF Mismatch (Yes)	CBV/CBF Mismatch (No)
C-arm ($n = 36$)	21	15
PCT ($n = 36$)	31	5

Note:—n = total number of CBV and CBF perfusion map pairs presented to all observers per modality.

Table 4: Kappa statistical evaluation for interobserver performance of ischemic lesion mismatch (CBF/CBV lesion size) detection for 3 independent observers

	κ Coefficient	Percentage Agreement	Statistical Significance
C-arm ($n = 12$)	0.31	66.6%	$P = .03$
PCT ($n = 12$)	0.07	77.7%	$P = .34$

Note:—n = total number of perfusion maps presented to a single observer.

Table 5: Summary of CBF measurements

	Ischemic Hemisphere	Normal Hemisphere
Mean C-arm CBF measurements	13.2 ± 7.4	40.3 ± 13.6
Mean PCT CBF measurements	3.9 ± 2.0	18.6 ± 7.7

Note:—All values are listed in units of mL/100 g/s.

Table 6: Summary of CBV measurements

	Ischemic Hemisphere	Normal Hemisphere
Mean C-arm CBV measurements	1.6 ± 0.9	4.9 ± 1.6
Mean PCT CBV measurements	0.8 ± 0.5	2.0 ± 0.6

Note:—All values are listed in units of mL/100 g.

crease with higher measured CBF and CBV values. The line fit of the data are plotted on each Bland-Altman plot to illustrate this trend of the C-arm CT perfusion region-of-interest measurements.

C-arm CT and PCT exhibited an agreement in 10 of 12 regions of interest (83%) of a CBF reduction in the ischemic hemisphere (relative to the normal hemisphere) of at least 50%. An agreement was found in 7 of 12 regions of interest (58%) for the CBV measurement.

DISCUSSION

The goal of this study was to evaluate the feasibility of performing measurements of CBV and CBF with the use of a novel high-speed 3D acquisition on a flat detector C-arm angiographic system (with PCT used as a criterion standard), in a canine stroke model. Statistical analysis of the region-of-interest data indicates a good correlation between C-arm CT and PCT measured perfusion values, with the C-arm CT tending to overestimate the measured perfusion value (both CBV and CBF) relative to PCT (Fig 4). Our qualitative analysis also demonstrates similar interobserver agreement between the C-arm CT and PCT modalities for both lesion detection and identification of perfusion mismatch.

The statistical results from the observer-based lesion detection study (Table 2) indicate that there is substantial to almost perfect agreement among the observers for detection and location of the ischemic lesions for both the PCT and C-arm CT perfusion maps. An interobserver agreement of 100% was found for the lesion identification on C-arm CT maps, indicating that C-arm CT maps are relatively easy to read and interpret.

The statistical results from the observer-based mismatch detection study (Table 4) indicate that the interobserver agreement for mismatch identification (as measured by the κ coefficient) is significantly less than for the lesion detection. Despite the relatively low κ coefficients, the readers show a similar percentage agreement between PCT and C-arm modalities for the mismatch study, indicating that the observers had similar interpretations of the maps for both C-arm and PCT modalities. One well-known drawback of the κ statistic is the loss of significance when measuring agreement between observers in cases with a rare number of findings.[18] It is important to note that observers identified a small number of cases with no mismatch (Table 3) for both the C-arm maps ($n = 15$) and the PCT maps ($n = 5$). It is likely that the κ statistic is unfairly penalized as a result of this issue.

Three factors help to explain limitations of the C-arm CT acquisition and the lack of agreement seen in the measurements of CBV and CBF obtained with C-arm CT and PCT. First, it is well documented that because of limitations in low contrast resolution, the current commercially available flat detector C-arm CT systems are not capable of tissue contrast at the level of accuracy and sensitivity that is possible with the use of standard diagnostic CT; the limit of C-arm CT contrast resolution is approximately 10 HU for the highest-quality scan protocols.[19-21] Many standard CT perfusion protocols are performed with the use of injections of 40–60 mL of contrast agent at a rate of 4–5 mL/s. This results in time enhancement curves for arteries and veins that often peak on the order of several hundreds of HU (or more) relative to the baseline. The contrast resolution of C-arm CT is sufficiently sensitive to measure intensity values of this magnitude for arterial and venous anatomic structures. However, with the use of such an injection protocol, the time enhancement curves in normal parenchyma (white/gray matter) often peak at <20 HU (relative to baseline) and even less in the ischemic tissue.[22] These levels are just at the limit of the contrast resolution of currently available C-arm CT detectors. The experimental high-speed C-arm CT protocol used in our study captured only 133 projection images during each of the 7 rotations, and this undersampled acquisition further limits the contrast resolution as compared with the highest-quality C-arm CT scans, which acquire almost 500 projections over a period of 20 seconds. Second, the lower temporal resolution (in addition to the applied smoothing kernels) of the C-arm CT results in an interpolated time attenuation curve that is broader and peaks significantly lower when compared with conventional CT, an effect more pronounced for arterial voxels (Fig

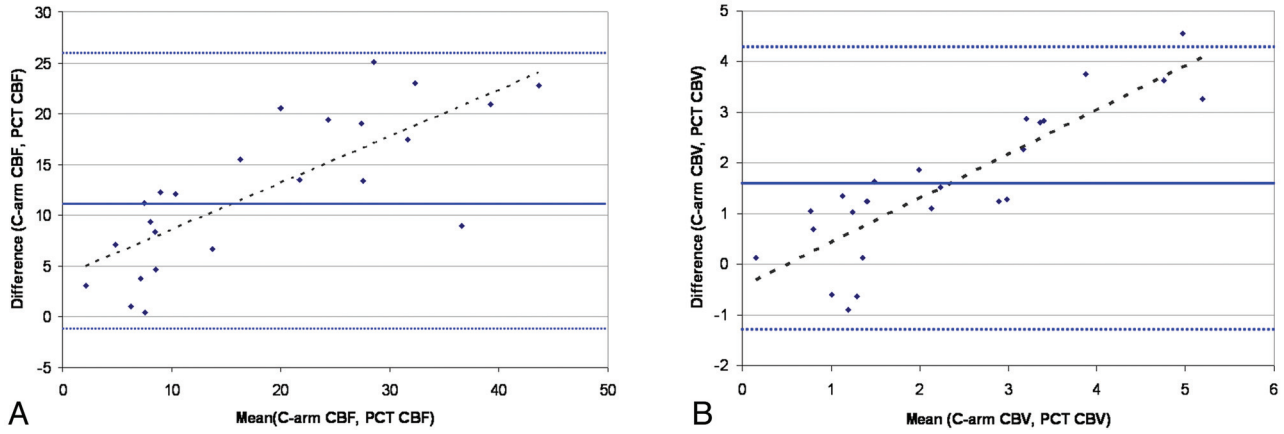

FIG 4. *A,* Bland-Altman analysis of CBF measurements; *B,* Bland-Altman analysis of CBV measurements.

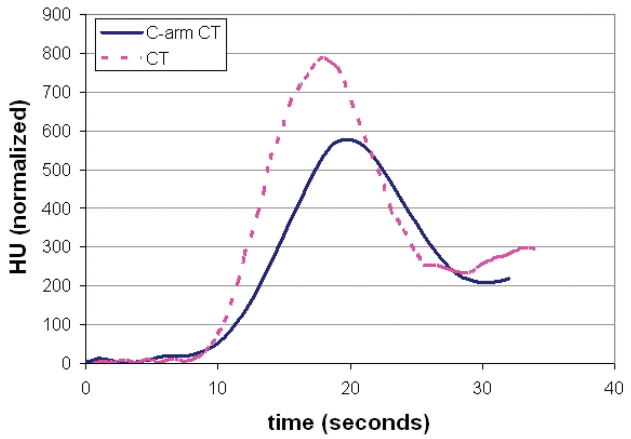

FIG 5. CBF overestimation by C-arm CT primarily caused by differences in AIF measurements between PCT and C-arm CT.

5). As a result, the underestimated arterial AIF curve enhancement level inversely impacts the global scaling of the perfusion parameters and thus introduces our overestimation of these values. Third, at the time of the study, the C-arm system was limited to a maximum of 7 bidirectional rotations, which resulted in a window of data acquisition that was limited to 33.6 seconds from the start of the injection. Because of the canine's relatively fast circulation times, this constraint presented truncation of TAC data for only the ischemic regions of the brain and probably was a factor in the lower number of identified perfusion mismatches for the C-arm perfusion maps compared with PCT (Table 3). This limited temporal window probably would present issues for TAC measurement in humans for both normal and ischemic tissue because of the relatively slower circulation times relative to that of the canine.

To compensate somewhat for the lack of contrast resolution, contrast was injected at a higher rate for the C-arm CT studies than what was used for the standard PCT (3.5 mL/s versus 2 mL/s). This provided a higher level of peak enhancement in the parenchyma and simultaneously allowed us to minimize the differences in the total duration (length) of the contrast bolus as compared with that used for PCT. In further efforts to maximize contrast resolution SNR was improved in the images by use of a smooth kernel for reconstruction (noise reduction) and by performing additional smoothing along the sections (z-direction). Whereas these smoothing algorithms do provide increased SNR for the parenchyma, the smoothing operation removes high spatial frequency content such that the true HU measurements are no longer maintained. This (combined with the low temporal sampling of C-arm CT) causes the issue of underestimation of the Hounsfield level measurements of the arterial curves (Fig 5) and can result in the overestimation of parenchymal enhancement in the vicinity of highly enhancing arteries and veins.

The fastest commercial C-arm CT acquisition protocols are typically ≥6 seconds for a temporal series of 3D acquisitions. Our prototype high-speed rotational protocol increased the speed of the gantry rotation so that it allowed a temporal sampling rate of 4.3 seconds. Wintermark et al[7] performed a systematic in vivo evaluation of the impact of varying temporal sampling rates for PCT measurements and found that there was a significant increase in measured values for CBV and CBF as the temporal resolution decreased beyond 1 sample every 3 seconds (based on a total volume of 40 mL injected at 4 mL/s). These findings are in line with our C-arm CT measurements (acquired at 1 sample every 4.3 seconds) of CBF and CBV because our measurements consistently overestimated these values relative to PCT (acquired at 1 sample per second) and led us to conclude that the overestimation for C-arm CT CBV and CBF parameters is primarily caused by low sampling frequency.[7]

Wintermark et al[7] also showed that injecting contrast for a longer duration, while by using the same injection rate, can effectively widen the contrast bolus. This can also help to compensate for a lack of temporal resolution. They were able to achieve quantitatively accurate measurements with a temporal sample rate of 1 sample every 4 seconds simply by increasing the total volume of the contrast from 40 mL to 60 mL. This would indicate that a similar strategy could potentially be applied to perfusion measurements performed with a C-arm CT protocol as one method to compensate for the limitations in temporal resolution. This was not performed in our study because the C-arm CT system was limited to a maximum of 7 bi-directional rotations (total scan time of 28.6 seconds). This limitation thus prevented us from further increasing the injection duration because severe truncation of the enhancement curves would occur.

Ongoing improvements to both system hardware (detector

and C-arm gantry) and processing algorithms are likely to further improve the contrast resolution limitations with the current high-speed C-arm CT acquisitions. The next generation of flat detectors will exhibit increased readout rates (allowing for more projections and faster acquisition times), increased contrast sensitivity, and increased bit depth, which will all lead to reconstructions with superior SNR to currently available systems. Software algorithms such as edge-preserving bi-lateral filters,[23] iterative reconstruction techniques,[24] compressed sensing algorithms,[25] and many other state-of-the-art image processing and image reconstruction algorithms must be evaluated to further optimize the image quality and quantitative accuracy of this technique.

Future engineering improvements in the C-arm gantry as well as the control and data acquisitions systems are necessary to improve temporal resolution limitations by shortening the delay time between rotations and further increasing speed of the C-arm rotation. Additional engineering efforts are also necessary to allow for series of bidirectional acquisitions that can extend up to 50 seconds from the start of the injection to prevent truncation of the TAC curves in the ischemic regions of the brain.

At the time of the study, the prototype and visualization software had not yet been optimized to generate and process high-quality MTT and TTP maps. Future work will also include the generation and evaluation of the full suite of cerebral perfusion parameters with C-arm CT perfusion imaging protocols. A comparison of radiation dose was also not considered for this study, and further studies must be performed to optimize and characterize the radiation dose to the patient with the C-arm CT perfusion imaging technique. Flat detector C-arm CT also provides the possible advantage of whole-brain perfusion imaging because the field of view is adequate to image the entire human brain with each rotational acquisition and should be considered for evaluation in future studies.

This study has shown the feasibility of acquiring dynamic cerebral perfusion measurements with the use of C-arm CT on a commercially available angiography system. This technology has the potential to provide physicians with the ability to evaluate both the physiologic state and vascular anatomic details of a patient in the angiography suite before, during, and after an intervention. Furthermore, this technology takes us 1 step closer to providing the necessary tools that will allow suitable patients with acute ischemic stroke to be taken directly from the emergency department to the interventional suite for diagnosis, triage, and treatment, potentially saving significant amounts of time otherwise spent in transport to and from diagnostic imaging modalities.

CONCLUSIONS

Qualitative and semi-quantitative measurements of CBF and CBV with the use of a C-arm CT system and a single intravenous injection of contrast agent are feasible. Further imminent improvements in C-arm system design, detector sensitivity and readout rates, and software algorithms seem likely to improve the ability to accurately measure (quantify) perfusion parameters by using flat detector angiographic systems. Availability of these tools has the potential to allow for a decrease in time to revascularization and further assessment of physiologic changes in patients with stroke during treatment in the angiographic suite.

ACKNOWLEDGMENTS

We thank our colleagues, Dr Beverly Aagaard-Kienitz and Dr David Niemann, who reviewed and scored the CBF and CBV maps.

Disclosures: Kevin Royalty—*RELATED: Grant:* Siemens Medical Solutions USA,* Comments: Funding for project was provided by Siemens; *UNRELATED: Employment:* Siemens Medical Solutions USA; OTHER RELATIONSHIPS: Full-time PhD student at University of Wisconsin Department of Biomedical Engineering. Michael Manhart—*RELATED: Grant:* Siemens AG, Angiography & Interventional X-Ray Systems, Forchheim, Germany.* Yu Deuerling-Zheng—*UNRELATED: Employment:* Siemens Healthcare. Charles Strother—*RELATED: Grant:* Siemens Healthcare,* Comments: Master Research agreement with UW; *Support for Travel to Meetings for the Study or Other Purposes:* Siemens Healthcare (under the Master Research agreement with UW), Comments: For scientific peer-reviewed meeting presentations; *UNRELATED: Other:* Payment for IP licensed by Siemens Healthcare. Andreas Fieselmann—*UNRELATED: Employment:* Siemens AG (**money paid to institution*).

REFERENCES

1. Lees KR, Hankey GJ, Hacke W. **Design of future acute-stroke treatment trials.** *Lancet Neurol* 2003;2:54–61
2. Struffert T, Deuerling-Zheng Y, Kloska S, et al. **Cerebral blood volume imaging by flat detector computed tomography in comparison to conventional multislice perfusion CT.** *Eur Radiol* 2010;21:882–89
3. Struffert T, Deuerling-Zheng Y, Kloska S, et al. **Flat detector CT in the evaluation of brain parenchyma, intracranial vasculature, and cerebral blood volume: a pilot study in patients with acute symptoms of cerebral ischemia.** *AJNR Am J Neuroradiol* 2010;31:1462–69
4. Ahmed AS, Zellerhoff M, Strother CM, et al. **C-arm CT measurement of cerebral blood volume: an experimental study in canines.** *AJNR Am J Neuroradiol* 2009;30:917–22
5. Bley T, Strother CM, Pulfer K, et al. **C-arm CT measurement of cerebral blood volume in ischemic stroke: an experimental study in canines.** *AJNR Am J Neuroradiol* 2010;31:536–40
6. Yasuda R, Royalty K, Pulfer K, et al. **C-arm CT measurement of cerebral blood volume using intra-arterial injection of contrast medium: an experimental study in canines.** *AJNR Am J Neuroradiol* 2012;33:1696–1701
7. Wintermark M, Smith WS, Ko NU, et al. **Dynamic perfusion CT: optimizing the temporal resolution and contrast volume for calculation of perfusion CT parameters in stroke patients.** *AJNR Am J Neuroradiol* 2004;25:720–29
8. Ganguly A, Fieselmann A, Marks M, et al. **Cerebral CT perfusion using an interventional C-arm imaging system: cerebral blood flow measurements.** *AJNR Am J Neuroradiol* 2011;32:1525–31
9. Mordasini P, El-Koussy M, Brekenfeld C, et al. **Applicability of table-side flat panel detector CT parenchymal cerebral blood volume measurement in neurovascular interventions: preliminary clinical experience.** *AJNR Am J Neuroradiol* 2011;33:154–58
10. Zellerhoff M, Deuerling-Zheng Y, Strother CM, et al. **Measurement of cerebral blood volume using angiographic C-arm systems.** *Proc. SPIE* 7262, Medical Imaging 2009: Biomedical Applications in Molecular, Structural, and Functional Imaging, 72620H (February 27, 2009)
11. Van der Bom IMJ, Mehra M, Walvick RP, et al. **Quantitative evaluation of C-Arm CT cerebral blood volume in a canine model of ischemic stroke.** *AJNR Am J Neuroradiol* 2012;33:353-58
12. Fieselmann A, Ganguly A, Deuerling-Zheng Y, et al. **A dynamic reconstruction approach for cerebral blood flow quantification with an interventional C-arm CT.** *2010 IEEE International Symposium on Biomedical Imaging: From Nano to Macro* 2010:53–56
13. Fieselmann A, Ganguly A, Deuerling-Zheng Y, et al. **Interventional 4-D C-arm CT perfusion imaging using interleaved scanning and partial reconstruction interpolation.** *IEEE Trans Med Imaging* 2012;31:892–906

14. Kudo K, Sasaki M, Yamada K, et al. **Differences in CT perfusion maps generated by different commercial software: quantitative analysis by using identical source data of acute stroke patients.** *Radiology* 2010;254:200–09
15. Konstas AA, Goldmakher GV, Lee TY, et al. **Theoretic basis and technical implementations of CT perfusion in acute ischemic stroke, part 2: technical implementations.** *AJNR Am J Neuroradiol* 2009;30:885–92
16. Wellens D, Wouters L, De Reese R, et al. **The cerebral blood distribution in dogs and cats: an anatomical and functional study.** *Brain Res* 1975;86:429–38
17. Vierra AJ, Garrett JM. **Understanding interobserver agreement: the kappa statistic.** *Fam Med* 2005;37:360–61
18. Feinstein AR, Cicchetti DV. **High agreement but low kappa: I. The problems of two paradoxes.** *J Clin Epidemiol* 1990;43:543–49
19. Struffert T, Richter G, Engelhorn T, et al. **Visualisation of intracerebral haemorrhage with flat-detector CT compared to multislice CT: results in 44 cases.** *Eur Radiol* 2009;19:619–25
20. Kalender WA. **Der Einsatz von Flachbilddetektoren für die CT-Bildgebung.** *Der Radiologe* 2003;43:379–87
21. Loose R, Wucherer M, Brunner T. **Visualization of 3D low contrast objects by CT cone-beam reconstruction of a rotational angiography with a dynamic solid body detector.** *RoFo* 2005;S1:PO 160
22. Silvennoinen HM, Hamberg LM, Valanne L, et al. **Increasing contrast agent concentration improves enhancement in first-pass CT perfusion.** *AJNR Am J Neuroradiol* 2007;28:1299–303
23. Manduca A, Yu L, Trzasko JD, et al. **Projection space denoising with bilateral filtering and CT noise modeling for dose reduction in CT.** *Med Phys* 2009;36:4911–19
24. Supanich, M, Tao Y, Nett B, et al. **Radiation dose reduction in time-resolved CT angiography using highly constrained back projection reconstruction.** *Phys Med Biol* 2009;54:4575–93
25. Nett BE, Brauweiler R, Kalender W, et al. **Perfusion measurements by micro-CT using prior image constrained compressed sensing (PICCS): initial phantom results.** *Phys Med Biol* 2010;55:2333–50